Mechanism of Biologically Relevant Deoxygenation of Dimethyl Sulfoxide Coupled with Pt(II) to Pt(IV) Oxidation of Orthoplatinated Oximes. Synthetic, Kinetic, Electrochemical, X-ray Structural, and Density Functional Study

Larissa Alexandrova,[†,⊥] Oleg G. D'yachenko,[‡] Grigory M. Kazankov,[‡] Vladimir A. Polyakov,[§] Pavel V. Samuleev,[‡] Enrique Sansores,[†] and Alexander D. Ryabov*[,‡]

Contribution from the Instituto de Investigaciones en Materiales, UNAM, Circuito Exterior s/n, Ciudad Universitaria, Apdo. Postal 70-360, Coyoacán CP 04510, México, D.F., Mexico, Department of Chemistry, M. V. Lomonosov Moscow State University, 119899 Moscow, Russia, and D. I. Mendeleev Moscow University of Chemical Technology, Miusskaya sq. 9, 125820 Moscow, Russia

Received December 13, 1999

Abstract: Orthometalated aryl oxime complexes *cis*-(*C,S*)-[Pt^{II}(C_6H_3-2-CMe═NOH-5-R)Cl(Me_2S═O)] (**1**, R = H (**a**), MeO, Me, F, and Cl) undergo deoxygenation of dimethyl sulfoxide (DMSO) in methanol in the presence of HCl to afford the Pt(IV) dimethyl sulfide complexes *fac*-[Pt^{IV}(C_6H_3-2-CMe═NOH-5-R)Cl_3(Me_2S)] (**2**), the composition of which was confirmed by an X-ray structural study of **2a**. The mechanism of the deoxygenation coupled with the oxidation of Pt(II) to Pt(IV) was investigated using cyclic voltammetry, UV−vis, and ^{1}H NMR spectrometry techniques at 40−60 °C in the presence of HCl, LiCl, and $NaClO_4$. The conversion of **1** into **2** does not occur intramolecularly and involves two time-resolved phases which were studied independently. The first is the substitution of chloride for DMSO to afford the anionic reactive complexes *cis*-[Pt(C_6H_3-2-CMe═NOH-5-R)Cl_2]$^-$ (**1**$_{Cl}$), which are involved in the acid-promoted interaction with free DMSO in the second phase. The formation of **1**$_{Cl}$ follows the usual two-term rate law $k_{obs1} = k_s + k_{Cl}$[LiCl], the k_{Cl}-driven pathway being negligible for the electron-rich complex with R = MeO. Thus-generated complexes **1**$_{Cl}$, in contrast to their precursors **1**, are more susceptible to oxidation, and the irreversible peak for **1**$_{Cl}$, $E(p1)$, is observed ca. 300 mV more cathodically compared to that of **1**. The second phase is acid-catalyzed and at low LiCl concentrations follows the rate expression $k_{obs2}[H^+]^{-1} = k_{10}' + k_{10}$[LiCl]. The complexes with the electron-withdrawing substituents R react faster, and there is a linear correlation between log k_{10} and $E(p1)$. The first-order in the acid is discussed in terms of two kinetically indistinguishable mechanisms involving the rate-limiting either electron transfer from **1**$_{Cl}$ to protonated DMSO (mechanism 1) or insertion of the S═O bond of free DMSO into the platinum−hydride bond of the reactive hydride complex of Pt(IV), *cis*-[Pt(C_6H_3-2-CMe═NOH)(H)Cl_2], to afford a {Pt−SMe_2−OH} fragment. Its protonation by HCl and dissociation of water gives the final product **2** (mechanism 2). ^{1}H NMR evidence is presented for the formation of the hydride species on protonation of a Pt(II) complex, whereas a density functional study of the two mechanisms indicates that mechanism 2 is less energy demanding. The system studied is viewed as a functioning mimetic of the Mo-dependent enzyme DMSO reductase because of several common features observed in catalysis.

Introduction

Metal-ion-mediated deoxygenation of sulfoxides into corresponding sulfides has recently attracted much attention in connection with its synthetic virtue,[1,2] the structural and mechanistic behavior of sulfoxide ligands in the coordination sphere of transition metal complexes,[3] and the biological deoxygenation of dimethyl sulfoxide catalyzed by the molybdenum-dependent enzyme.[4] Since the pioneering work of Kukushkin et al.,[5] much effort has been devoted to the investigation of the deoxygenation promoted by acido and related complexes of platinum(II), which is accompanied by the oxidation of Pt(II) into Pt(IV) (eq 1). The process shown

$$[Pt^{II}X_3(SOMe_2)]^- + 2HCl \rightarrow [Pt^{IV}Cl_2X_3(SMe_2)]^- + H_2O \quad (1)$$

by eq 1 has been demonstrated by several groups of authors[6−8] and confirmed by X-ray structural characterization of the

* Address correspondence to this author (temporary address) at Department of Chemistry, Carnegie Mellon University, 4400 Fifth Ave., Pittsburgh, PA 15213. Fax: (412) 268-1061. E-mail: ryabov@enz.chem.msu.ru.

† Ciudad Universitaria.

‡ M. V. Lomonosov Moscow State University.

§ D. I. Mendeleev Moscow University of Chemical Technology.

⊥ Visiting scientist at the Department of Chemistry, M. V. Lomonosov Moscow State University.

(1) Kukushkin, V. Y. *Usp. Khim.* **1990**, *59*, 1453−1468.

(2) Kukushkin, V. Y. *Coord. Chem. Rev.* **1995**, *139*, 375−407.

(3) Calligaris, M.; Carugo, O. *Coord. Chem. Rev.* **1996**, *153*, 83−154. Calligaris, M. *Croat. Chem. Acta* **1999**, *72*, 147−169.

(4) Weiner, J. H.; Rothery, R. A.; Sambasivarao, D.; Trieber, C. A. *Biochim. Biophys. Acta* **1992**, *1102*, 1−18.

(5) Kukushkin, Y. N.; Vyazmenskii, Y. E.; Zorina, L. I.; Pazukhina, Y. L. *Zh. Neorg. Khim.* **1968**, *13*, 1595−1599.

(6) Pakhomova, I. V.; Konovalov, L. V.; Komyagin, N. T.; Yanovsky, A. I.; Struchkov, Y. T. *Zh. Obsch. Khim.* **1988**, *58*, 733−738.

10.1021/ja994342k CCC: $19.00
Published on Web 05/17/2000

products formed. Nevertheless, reaction 1 seems to be mechanistically rather controversial, if one considers, for example, the known standard redox potentials of the corresponding half-reactions 2 and 3.

$$[PtCl_6]^{2-} + 2e \rightarrow [PtCl_4]^{2-} \qquad E_2^\circ \quad (2)$$

$$Me_2S{=}O + 2H^+ + 2e \rightarrow Me_2S + H_2O \qquad E_3^\circ \quad (3)$$

The values available, viz., E_2° and E_3° of 0.74[9] and 0.16 V (pH 7),[10] respectively, versus NHE indicate that reaction 1 is formally thermodynamically unfavorable, the uphill process with ΔG° ca. 110 kJ mol^{-1}. Thus, it was naïve to expect a simple reaction mechanism for the Pt(II)-induced deoxygenation of sulfoxides involving, for example, a transfer of two electrons from Pt(II) to S(IV). Rather, a nonconcerted, multistep pathway would have been anticipated, and our understanding of it could throw light on the mechanism of the related enzymatic reaction.[4]

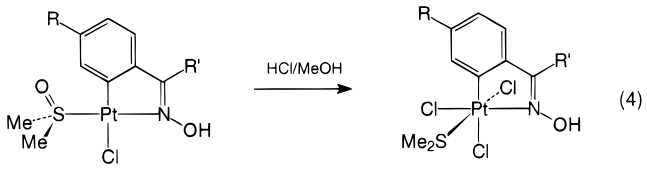

(4)

1 **2**

Complex	R	R'
a	H	Me
b	MeO	Me
c	Me	Me
d	F	Me
e	Cl	Me
f	H	n-C_7H_{15}
g	H	CHMeEt

It should, however, be mentioned that in contrast to the enzymatic deoxygenation, the Pt(II)-promoted reactions often proceed under harsh conditions. The formation of dimethyl sulfide occurs under reflux in the presence of high concentrations of HCl.[2] Our recent work suggested an approach to make the reaction conditions milder.[11] When 2-methyl-1-phenylbutan-1-one oxime was reacted with *cis*-[$PtCl_2(SOMe_2)_2$] in methanol, the major reaction product was the orthometalated Pt(IV) complex with coordinated dimethyl sulfide, formulated as **2g** on the basis of an X-ray structural investigation. Together with **2g**, a small amount of dimethyl sulfoxide Pt(II) complex **1g** was isolated, showing that **1** could be a precursor of **2**. Direct proof is gained in this work. Less bulky ring-substituted oxime complexes **1** have been shown to transform cleanly into dimethyl sulfide Pt(IV) complexes **2** in MeOH at 40−60 °C in the presence of a small amount of HCl. Reaction 4 afforded **2a** in good yield and provided an object for the mechanistic investigation of the deoxygenation of sulfoxides in the presence of Pt(II) complexes. Orthometalated complexes are superior for mechanistic studies[12] because of advantages utilized by us previously in studies of mechanisms of reactions of platinacycles.[13−17] First, the covalently σ-bound, substitutionally inert orthoplatinated ligand limits possible substitution and exchange processes at Pt(II). As a result, mechanistic information obtained by different techniques is more straightforward and easier to rationalize. Second, electron-donating or -withdrawing groups at the σ-bound aryl ring cause variations in the electronic features of the entire molecule, the steric properties being unaffected. Third, an orthoplatinated organic ligand is located in the Pt(II) plane, and there is no steric retardation for incoming ligands to approach the Pt(II) center. Apart from several special cases,[18−20] the attack occurs via associative mechanisms.[21,22] In addition, platinacycles **1** further demonstrate wide applicability of oxime ligands in the comprehensive coordination chemistry.[23,24] Thus, in this work we report on a detailed mechanistic, structural, and density functional study of reaction 1, using as an example the square-planar sulfoxide platina(II)cycles **1** which transform into octahedral Pt(IV) complexes **2**. The investigation includes synthesis of complexes **1** and **2**, an X-ray structural study of **2a**, spectral (UV−vis, ^{1}H NMR) and cyclic voltammetry (CVA) examination of **1** and **2** in the presence of LiCl and HCl, and a kinetic study of DMSO substitution for chloride in **1**, as well as of the acid-promoted formation of the final reaction products **2**. The mechanistic conclusions are discussed together with results of the quantum-chemical simulations using a density functional theory.

Results

Synthesis and Properties of Platina(II)cycles 1. Sulfoxide platinum(II) complexes **1** were prepared from the corresponding ring-substituted acetophenone oximes and *cis*-[$PtCl_2(SOMe_2)_2$][25] in refluxing methanol (30−36 h) as described in previous work for the unsubstituted oxime.[11] Platinacycles **1** precipitated from the reaction solution on cooling as spectrally pure yellow crystals. Isolated yields were usually 45−67% (Table 1). The somewhat lower yield for fluoro-substituted compound **1d** (23%) is probably due to its better solubility in MeOH. In the previous work, we have concluded that the steric effect is responsible

(7) Fanizzi, F. P.; Natile, G.; Maresca, L.; Manotti-Lanfredi, A. M.; Tiripicchio, A. *J. Chem. Soc., Dalton Trans.* **1984**, 1467−1470.
(8) Kukushkin, V. Y.; Belsky, V. K.; Konovalov, V. E.; Aleksandrova, E. A.; Pankova, E. Y.; Moiseev, A. I. *Phosphorus, Sulfur, Silicon* **1992**, *69*, 103−117.
(9) Bard, A. J.; Faulkner, L. R. *Electrochemical Methods. Fundamentals and Applications*; John Wiley & Sons: New York, 1980.
(10) Wood, P. M. *FEBS Lett.* **1981**, *124*, 11−14.
(11) Ryabov, A. D.; Kazankov, G. M.; Panyashkina, I. M.; Grozovsky, O. V.; Dyachenko, O. G.; Polyakov, V. A.; Kuz′mina, L. G. *J. Chem. Soc., Dalton Trans.* **1997**, 4385−4391.
(12) Canty, A. J.; van Koten, G. *Acc. Chem. Res.* **1995**, *28*, 406−413.
(13) Ryabov, A. D.; Kuz′mina, L. G.; Dvortsova, N. V.; Stufkens, D. J.; van Eldik, R. *Inorg. Chem.* **1993**, *32*, 3166−3174.
(14) Schmulling, M.; Ryabov, A. D.; van Eldik, R. *J. Chem. Soc., Dalton Trans.* **1994**, 1257−1263.
(15) Ryabov, A. D.; Kuz'mina, L. G.; Polyakov, V. A.; Kazankov, G. M.; Ryabova, E. S.; Pfeffer, M.; van Eldik, R. *J. Chem. Soc., Dalton Trans.* **1995**, 999−1006.
(16) Krooglyak, E. V.; Kazankov, G. M.; Kurzeev, S. A.; Polyakov, V. A.; Semenov, A. N.; Ryabov, A. D. *Inorg. Chem.* **1996**, *35*, 4804−4806.
(17) Gossage, R. A.; Ryabov, A. D.; Spek, A. L.; Stufkens, D. J.; van Beek, J. A. M.; van Eldik, R.; van Koten, G. *J. Am. Chem. Soc.* **1999**, *121*, 2488−2497.
(18) Frey, U.; Helm, L.; Merbach, A. E.; Romeo, R. *J. Am. Chem. Soc.* **1989**, *111*, 8161−8165.
(19) Romeo, R.; Alibrandi, G. *Inorg. Chem.* **1997**, *36*, 4822−4830.
(20) Romeo, R.; Plutino, M. R.; Elding, L.-I. *Organometallics* **1997**, *16*, 5909−5916.
(21) Basolo, F.; Pearson, A. G. *Mechanism of Inorganic Reactions. A Study of Metal Complexes in Solution*, 2nd ed.; Wiley: New York, 1967.
(22) Kotowski, M.; van Eldik, R. In *Substitution, Isomerization and Related Reactions of Four-Coordinate Complexes*; van Eldik, R., Ed.; Elsevier: Amsterdam, Oxford, New York, Tokyo, 1986; Vol. 7, pp 219−271.
(23) Kukushkin, V. Y.; Tudela, D.; Pombeiro, A. J. L. *Coord. Chem. Rev.* **1996**, *156*, 333−362.
(24) Kukushkin, V. Y.; Pombeiro, A. J. L. *Coord. Chem. Rev.* **1999**, *181*, 147−175.
(25) Ranatunge-Bandarage, P. R. R.; Robinson, B. H.; Simpson, J. *Organometallics* **1994**, *13*, 500−510.

Table 1. Yields, UV−Vis, and ^{1}H NMR ($CDCl_3$) Spectral Data for Platinacycles **1**

complex (R, yield, %)	UV−vis (MeOH)[a] (λ_{max} (ϵ, M^{-1} cm^{-1}))	^{1}H NMR ($CDCl_3$, J in Hz)				
		C−CH_3	S−CH_3	N−OH	R	Ar
1a (H, 67)	303 (5100), 319 (4800)	2.39 (J = 6.3)	3.54 J = 23.8)	10.15 (J = 6.6)	−	7.1−7.15 (m, H3−H5), 8.03 (d, J = 8, J_{Pt-H} 51)
	304,[b] 322[b]	2.44 (J = 6.4)[c]	3.58 (J = 24.8)	n. o.		7.0−7.35 (m, H3−H5), 8.0 (d, J = 8, J_{Pt-H} = 44)
1b (MeO, 45)	314 (5500), 326 (5800)	2.45 (J = 5.9)[c]	3.61 (J = 24.5)	n. o.	3.84 (OCH_3)	6.73 (dd, J = 8.4, 2.6, H4), 7.28 (d, J = 8.4, H3), 7.70 (d, J = 2.6, J_{Pt-H} = 57, H6)
1c (Me, 48)	308 (3900), 323 (4100)	2.37 (J = 6)	3.53 (J = 24)	10.04 (J = 6.4)	2.38 ($ArCH_3$)	6.95 (d, J = 8.1, H3), 7.06 (d, J = 8.1, H4), 7.86 (s, J_{Pt-H} = 48, H6)
1d (F, 23)	302 (4200), 317 (4100)	2.38 (J = 6.4)	3.54 (J = 24)	10.01 (J = 6)	−	6.83 (td, J_{HH} 2.6, J_{HF} = 8.4, H4), 7.2 (dd, H3), 7.82 (dd J_{HH} = 2.6, J_{HF} = 10.4, H6)
1e (Cl, 51)	306 (5800), 322 (5650)	2.37 (J = 6.1)	3.54 (J = 24.2)	10.10 (J = 6.1)	−	7.1−7.3 (m, H3, H4), 8.05 (d, J = 1.95, J_{Pt-H} = 55.2, H6)
3	307 (5400), 329 (5500), 370 sh, 308,[b] 332[b]					

[a] All complexes have a shoulder at ca. 350 nm. [b] Chloroform solvent. [c] Methanol-d_4 solvent.

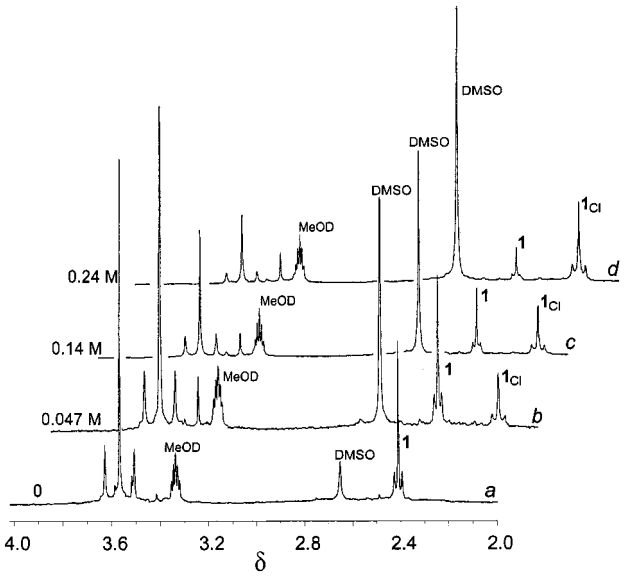

Figure 1. ^{1}H NMR spectra of complex **1a** obtained at different LiCl concentrations at 64 °C in methanol-d_4.

for the dominant formation of complex **2g**, whereas **1g** was isolated only in a very low yield.[11] In this study, we tested the long-chain phenyl *n*-heptyl ketone oxime as a sterically hindered but less bulky molecule. In accord with the previous proposal, formation of both **1f** and **2f** was observed. However, the reaction between *cis*-[$PtCl_2(SOMe_2)_2$] and phenyl *n*-heptyl ketone oxime is time-controlled, and complex **1f** is the only species that can be formed. Platinacycles **1** were characterized by UV−vis and ^{1}H NMR spectral data (Table 1). The structure of **1c** was confirmed by an X-ray single-crystal investigation.[26]

Reaction of 1 with LiCl. Complexes **1** react with LiCl in MeOH according to eq 5, which was investigated by ^{1}H NMR, cyclic voltammetry, and UV−vis techniques. The ^{1}H NMR

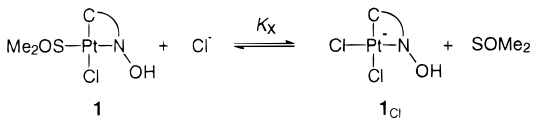

(5)

1 1_{Cl}

spectrum of **1a** (0.02 M) recorded in D_3COD at 64 °C contains extra resonances as compared to those in $CDCl_3$ (Figure 1). There is a weak singlet at δ 2.68 without Pt satellites from free DMSO, a strong resonance from coordinated DMSO at δ 3.58 (J_{PtH} = 25 Hz) (Figure 1a), and a weak signal around δ 3.55 with the satellites. The formation of free DMSO is ascribed to the minor product formed in eq 6a, since free DMSO is seen in the ^{1}H NMR spectrum of the methanolic solution of *cis*-[$PtCl_2$-$(SOMe_2)_2$], whereas the δ 3.55 signal is due to the solvolysis

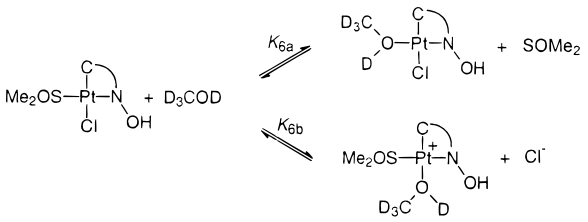

(6)

reaction 6b. Evidence for this is its disappearance on addition of 0.047 M LiCl. Added LiCl increases the fraction of unbound DMSO (δ 2.68) and gives rise to a new singlet at δ 2.19 (J_{PtH} = 10.2 Hz) (Figure 1b). There is an additional weak singlet at δ 3.42 (J_{PtH} = 22 Hz), the origin of which is not completely clear. It could tentatively be ascribed to the product formed in equilibrium 7. At 0.14 M LiCl (Figure 1c), the intensity of new

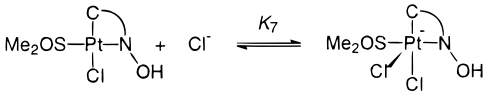

(7)

resonances at δ 2.19 and 2.68 increases further with a decrease of those at δ 2.44 (J_{PtH} = 6.4 Hz) and 3.58 from the oxime methyl and bound DMSO, respectively. The tendency holds at 0.24 M LiCl (Figure 1d). It should be mentioned that (i) the changes are rather fast at 64 °C and the spectrum does not practically fluctuate until next addition of LiCl and (ii) the signal intensities from the coordinated and free DMSO, as well as from the oxime methyls (δ 2.19 and 2.44), vary correspondingly. The spectral changes suggest that the substitution of chloride for DMSO (eq 5) is a dominant process under these conditions.

The electrochemical properties of platinacycles is a subject of independent interest,[27−32] and CVA was applied to **1a**−**e** (MeOH, 0.1 M $NaClO_4$, 25 and 55 °C). The voltammograms

(26) Revenco, M.; Alexandrova, L.; Ryabov, A. D. To be published.

(27) Headford, C. E. L.; Mason, R.; Ranatunge-Bandarage, P. R.; Robinson, B. H. *J. Chem. Soc., Chem. Commun.* **1990**, 601−603.
(28) Braterman, P. S.; Song, J.-I.; Wimmer, F. M.; Wimmer, S.; Kaim, W.; Klein, A.; Peacock, R. D. *Inorg. Chem.* **1992**, *31*, 5084−5088.
(29) Minghetti, G.; Pilo, M. I.; Sanna, G.; Seeber, R.; Stoccoro, S.; Laschi, F. *J. Organomet. Chem.* **1993**, *452*, 257−261.
(30) Kotler, A. N.; Puzyk, K. G.; Balashov, V. T. *Elektrokhimia* **1995**, *31*, 746−749.
(31) Crespo, M.; Grande, C.; Garcia, M. M.; Klein, A.; Font-Bardia, M.; Solans, X. *J. Organomet. Chem.* **1998**, *563*, 179−190.

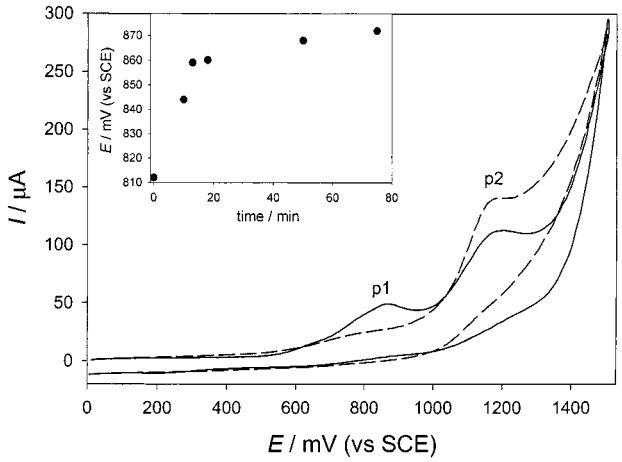

Figure 2. Cyclic voltammograms of complex **1a** in the absence (broken line) and 75 min after addition of 0.023 M LiCl (solid line) obtained at 55 °C, 0.1 M $NaClO_4$, [**1a**] 0.0006 M, at a scan rate 0.1 V s^{-1} in methanol solvent. (Inset) Variation of $E(p1)$ with time. For more details, see text.

Table 2. Oxidation Potentials $p1$ and $p2$ (in Volts) for Complexes **1** with and without 0.02 M LiCl in MeOH at 55 °C (0.1 M $NaClO_4$, SCE)

	in the absence of LiCl		in the presence of LiCl	
complex (R)	$p1$	$p2$	$p1$	$p2$
1a (H)	0.81[a]	1.18	0.875	1.20
1c (Me)	n.o.	1.17	0.83	1.17
1d (F)	0.88[a]	1.17	0.905	1.26 (shoulder)
1b (MeO)	n.o.	1.04; 1.40	0.785	1.03; 1.14
1e (Cl)	n.o.	1.26	0.93	1.25

[a] Poorly resolved.

for **1a** with and without added LiCl are shown in Figure 2. There is one irreversible oxidation peak, $p2$, around 1.2 V (versus SCE), together with a poorly resolved shoulder, $p1$, at ca. 0.8 V at [LiCl] = 0 (broken line). Addition of LiCl (0.02 M) develops the oxidation peak $p1$. Its position is time-dependent (inset to Figure 2), and a constant value is reached after 10−15 min at 55 °C. The final voltammogram (solid line) contains two irreversible peaks, $p1$ and $p2$, at 0.87 and 1.2 V, which are ascribed to the 2e oxidations of $\mathbf{1a}_{Cl}$ and **1a**, respectively, plausibly via transient Pt(III) complexes.[33] The LiCl-induced effects are fully consistent with eq 5. The CVA data suggest that, in contrast to neutral complexes **1**, anionic species $\mathbf{1}_{Cl}$ undergo oxidation at ca. 300 mV more negative potentials. Ring-substituted complexes **1b**−**e** were similarly tested, and the $p1$ and $p2$ values are given in Table 2. The $p1$ values for $\mathbf{1}_{Cl}$ depend on the nature of R, and the peak potentials are more cathodic for the electron-rich complexes, the largest difference being 145 mV for **1b** and **1e**.

Reaction 5 is observed by UV−vis spectroscopy (Figure 3). In MeOH as solvent, complex **1a** shows two absorption maxima at 303 and 319 nm, together with a broad plateau at 350 nm. Addition of LiCl develops a band at 350 nm, and the maxima at 303 and 319 nm diminish their intensity. Isosbestic points at 282 and 328 nm suggest that two absorbing species dominate in solution. The solvento species[17] (eq 6b) plays no important role here. To give more evidence for this, the structural analogue of **1a**, *trans*-(*N*,*N*)-[Pt^{II}(C_6H_4-2-CMe═NOH)Cl(py)] (**3**), was prepared and investigated by UV−vis spectroscopy. The spectra

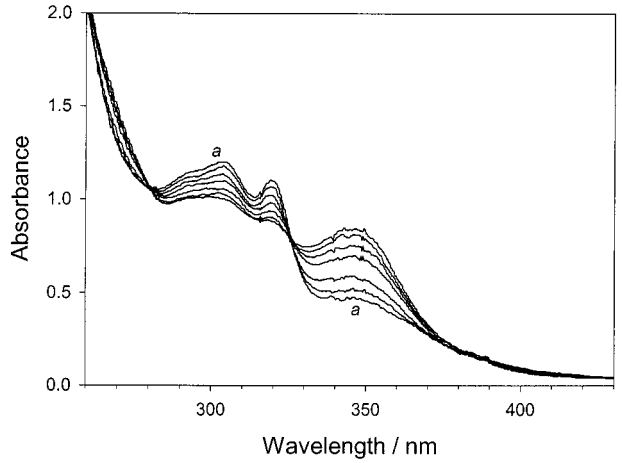

Figure 3. Spectral changes of complex **1a** (0.00025 M) with time in the presence of 0.005 M LiCl at 60 °C in MeOH. Spectrum a was recorded at time $t = 0$ after addition of LiCl; other spectra were obtained at t = 5, 15, 35, 50, 80, and 140 min, respectively.

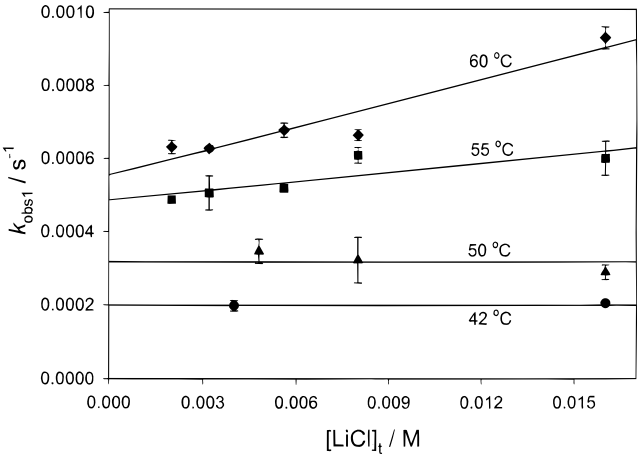

Figure 4. Pseudo-first-order rate constants k_{obs1} as a function of LiCl concentration for the substitution of chloride for dimethyl sulfoxide in complex **1a** at different temperatures in methanol solvent.

of **1a** and **3** recorded in $CHCl_3$ are similar (Table 1). More important is that their spectra in $CHCl_3$ and MeOH are also similar. Additionally, the spectrum of **3** in MeOH is practically insensitive to LiCl at 0.001−5.0 M, even at 55 °C, proving the insignificance of eq 6b.

The LiCl-induced absorbance changes depend on the concentration of LiCl added and can be reversed by addition of extra DMSO after the equilibration of **1a** with LiCl. An attempted isolation of $\mathbf{1a}_{Cl}$ after the methanol solution of **1a** was refluxed in the presence of a 10-fold excess of LiCl for 30 h resulted, after cooling, in a quantitative recovery of **1a**, confirming the reversible nature of eq 5.

Equilibria and Kinetics of Substitution of DMSO by Cl^- in Complexes 1. The kinetics of reaction 5 was studied as a function of the LiCl, $NaClO_4$, and HCl concentrations in MeOH at 42−60 °C. It was monitored at 353 nm for all complexes, except for **1b** (327 nm), at $[LiCl]_t \gg [\mathbf{1}]$ to ensure the pseudo-first-order conditions. The values of k_{obs1} were evaluated at different concentrations of $NaClO_4$ (0−0.1 M), HCl (0.005−0.05 M), and LiCl (0.003−0.02 M). The rate constants k_{obs1} were insensitive to $NaClO_4$ and HCl concentrations. The dependence of k_{obs1} on [LiCl] is demonstrated in Figure 4. As can be seen, the k_{obs1} is practically independent of [LiCl] at 42 and 50 °C, whereas the LiCl-dependent pathway manifests at higher temperatures, viz., 55 and 60 °C. These facts are in

(32) Balashev, K. P.; Puzyk, M. V.; Kotlyar, V. S.; Kulikova, M. V. *Coord. Chem. Rev.* **1997**, *159*, 109−120.
(33) Bandoli, G.; Caputo, P. A.; Intini, F. P.; Sivo, M. F.; Natile, G. *J. Am. Chem. Soc.* **1997**, *119*, 10370−10376.

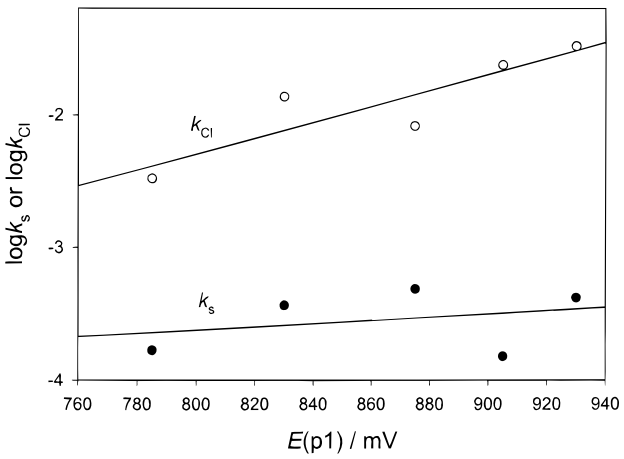

Figure 5. Dependencies of log k_s and log k_{Cl} on the $E(p1)$ potential for the substitution of chloride for dimethyl sulfoxide in complexes **1** at 55 °C in methanol solvent.

agreement with the accepted scheme for the ligand substitution in square-planar complexes,[21,34] according to which the rate law is given by eq 8. Here, k_{Cl} refers to the chloride-dependent

$$k_{obs1} = k_s + k_{Cl}[LiCl] \quad (8)$$

substitution pathway. Since the reaction rate is independent of chloride concentrations in several cases (Figure 4 and Figure 1S in the Supporting Information), k_s is the sum of the rate constants for the reversible reaction and the solvent-dependent substitution pathway; thus, the relative contribution of each path is difficult to estimate. Likely, the latter dominates, since reaction 5 proceeds at appreciable rates even when zero-order in LiCl holds. The rate law 8 is valid for ring-substituted complexes (Figure 1S), and the rate constants k_s and k_{Cl} for **1a**−**e** are summarized in Table 3. These do not correlate with the Hammett σ constants, presumably due to the fact that the R group affects the metal center via two channels, viz., the covalent σ-Pt−C and coordinative Pt←N bonds, the contribution of each being difficult to take into account.[35] Therefore, some other effective parameter related to the electronic density at the entire complex could be more useful. Such proved to be the $p1$ peak potentials for $\mathbf{1}_{Cl}$ (Table 2). As can be seen in Figure 5, there is a correlation between log k_{Cl} and $E(p1)$, with the anticipated positive slope of 6 ± 2 V^{-1}, since the electron-deficient compounds should react faster with the negatively charged incoming ligand. The slope is much lower for log k_s (1 ± 2 V^{-1}). The pathway is less electronically sensitive to the electroneutral solvent molecule. The activation enthalpy ($\Delta H_s^{\ddagger}$) and entropy ($\Delta S_s^{\ddagger}$) for the k_s pathway were calculated from the linear ln(k_s/T) versus T^{-1} plot for **1a** (Figure 2S, Supporting Information). The numerical values are given in Table 3.

The calculation of k_{obs1} using the nonlinear least-squares curve-fitting provided the infinite absorbances (A_∞) at a given concentration of LiCl. These were dependent on [LiCl] added (Figure 5S, Supporting Information) and were used for estimating the equilibrium constant K_x (eq 5). The dissociation of LiCl in MeOH should be taken into account, the K_{LiCl} for which equals 1.58 × 10^{-2} M,[36] since the experimental data were evaluated at $[LiCl]_t$ lower than 0.02 M. As in our previous work,[37] the equilibrium concentrations of Cl^- were calculated using the K_{LiCl} which were then used in the fitting of the data to eq 9 (for evaluation of eq 9, see Appendix). Here, A_o is the

$$(A_\infty - A_o) = \Delta\epsilon\left(\sqrt{0.25K_x^2[Cl^-]^2 + [Pt]_tK_x[Cl^-]} - \frac{K_x[Cl^-]}{2}\right) \quad (9)$$

initial absorbance, $\Delta\epsilon$ is the difference in the extinction coefficients for $\mathbf{1}_{Cl}$ and **1**, $[Pt]_t$ is the total concentration of Pt(II), and $[Cl^-]$ is the calculated equilibrium concentration of chloride. The data such as those in Figure 3S (Supporting Information) were fitted to eq 9, and the best-fit values of K_x were equal to 0.15 ± 0.05, 0.17 ± 0.06, and 0.19 ± 0.12 at 50, 55, and 60 °C, respectively. The equilibrium constants increase slightly with the temperature, the reaction enthalpy $\Delta H°$ being 10.6 ± 0.2 kJ mol^{-1} (calculated from the ln K_x versus T^{-1} plot; $\Delta S° = 25$ ± 1 J K^{-1} mol^{-1}).

Table 3. Kinetic Parameters k_s and k_{Cl} for the Substitution of Chloride for DMSO in Complexes **1** (Eq 8) and k_{10} and k_{10}' for the Conversion of **1** into **2** (Eq 10) in MeOH

complex (R)	T, °C	10^4k_s, s^{-1}	10^2k_{Cl}, M^{-1} s^{-1}	$10^2k'_{10}$, M^{-1} s^{-1}	k_{10}, M^{-2} s^{-1}
1a (H)	42	2.00 ± 0.16[a]	~0		
	50	3.2 ± 0.28	~0		
	55	4.87 ± 0.28	0.83 ± 0.33	2.4 ± 0.2	0.37 ± 0.07
	60	5.5 ± 0.3	2.2 ± 0.3		
1c (Me)	55	3.67 ± 0.3	1.4 ± 0.3	2.4 ± 0.1	0.29 ± 0.02
1d (F)	55	1.52 ± 0.28	2.38 ± 0.25	2.97 ± 0.03	0.48 ± 0.01
1b (MeO)	55	1.40 ± 0.03	0.55 ± 0.03	1.9 ± 0.1	0.10 ± 0.02
1e (Cl)	55	4.17 ± 0.03	3.28 ± 0.33	3.3 ± 0.1	0.70 ± 0.03

[a] $\Delta H_s^{\ddagger}$ = 24.5 ± 2.8 kJ mol^{-1}, $\Delta S_s^{\ddagger}$ = −81 ± 14 J K^{-1} mol^{-1}.

Protonation of Complex 1c. To demonstrate the ability of Pt(II) complexes **1** to generate the Pt(IV) hydride species on interaction with strong acids, complex **1c**, as the most electron-rich one with the lowest number of oxygen atoms, was treated with triflic acid in methanol. Compound **1c** (2.5 mg) was reacted with 15 μL of the acid in 1 mL of CH_3OH for 15 min. The solvent was then removed in a vacuum, and the ^1H NMR spectrum of the residue was recorded immediately after addition of dry methanol-d_4 showed the characteristic resonance at δ −14.8 with J_{PtH} = 1180 Hz. Its integral intensity corresponded to one proton as compared with other signals, which were found to have chemical shifts similar to those of the parent complex **1c**, and decreased with time due to instability of the compound and/or exchange of the hydride with deuterium atoms from the solvent.

Preparation of Complexes 2 from 1 in the Presence of HCl in MeOH. Sulfoxide Pt(II) complexes **1** transform readily into Pt(IV) sulfide complexes **2** in the MeOH−HCl system. The reaction usually takes 5−6 h, and the product precipitates from the solution on cooling. No additional crystallization is needed for purification. Complexes **2** were characterized by the analytical and ^1H NMR data, whereas the structure of **2a** was confirmed by a single-crystal X-ray structural study.

The ^1H NMR spectrum of **2a** recorded in $CDCl_3$ is simple compared to that of its analogue **2g** reported previously.[11] It consists of three methyl resonances at δ 2.20, 2.62, and 2.73 with ^{195}Pt satellites. The Pt−H coupling constants equal 40, 35.5, and 8.6 Hz, respectively, indicating that the former two refer to the diastereotopic methyls of coordinated Me_2S and the complex has no plane of symmetry. The signal at δ 2.73 is ascribed to the methyl group of acetophenone oxime. It is worth

(34) Wilkins, R. G. *Kinetics and Mechanism of Reactions of Transition Metal Complexes*, 2nd ed.; VCH: Weinheim, 1991.
(35) Ryabov, A. D. *Chem. Rev.* **1990**, *90*, 403−424.
(36) Janz, C. J.; Tomkins, R. P. T. *Nonaqueous Electrolytes Handbook*; Academic Press: New York, 1972.
(37) Ferstl, W.; Sakodinskaya, I. K.; Beydoun-Sutter, N.; Le Borgne, G.; Pfeffer, M.; Ryabov, A. D. *Organometallics* **1997**, *16*, 411−418.

Table 4. Yields and ^{1}H NMR ($CDCl_3-D_3COD$) Spectral Data for Platinacycles **2**

complex (R)	isolated yield, %	^{1}H NMR C−CH_3	S−CH_3	R	Ar
2a (H)	72	2.73 (J = 8.6)[a]	2.20 (J = 40.0), 2.62 (J = 35.5)	−	7.34−7.45 (m, H3−H5), 7.88 (d, J = 8, J_{Pt-H} = 23.4, H6)
		2.74 (J = 8.7)[b]	2.24 (J = 40.2), 2.35 (J = 38.8)	−	7.2−7.6 (m, H3−H5), 7.87 (d, J = 7.5, J_{Pt-H} = 25.6, H6)
2b (MeO)	34	2.57 (J = 8.3)	2.15 (J = 40.0), 2.40 (J = 37.1)	3.81 (OCH_3)	6.74 (dd, J = 8.54, 2.44, H4), 7.23 (d, J = 8.54, H3), 7.28 (d, J = 2.44, J_{Pt-H} = 30, H6)
2c (Me)	48	2.72 (J = 8.0)	2.25 (J = 40.6), 2.53 (J = 36.7)	2.49 ($ArCH_3$)	7.16 (d, J = 7.8, H4), 7.30(d, J = 7.8, H3), 7.66 (s, J_{Pt-H} = 28, H6)
2d (F)	21	2.78 (J = 8.6)	2.32 (J = 40.5), 2.53 (J = 37.7)	−	7.14 (ddd, J_{HH} = 8.3, 0.4, J_{HF} = 8.1, H3), 7.58 (dd, J_{HH} = 8.3, 1.5, J_{HF} = 8.1, H4), 7.59 (ddd, J_{HH} = 1.5, J_{HF} = 8.1, J_{Pt-H} = 28, H6)
2e (Cl)	43	2.75 (J = 8.0)	2.29 (J = 40.0), 2.53 (J = 36.4)	−	7.38−7.41 (m, H3, H4), 7.85 (d, J_{HH} = 2, J_{PtH} = 28, H6)

[a] In $CDCl_3$ as solvent, δ(NOH) 11.1. [b] In pure methanol-d_4.

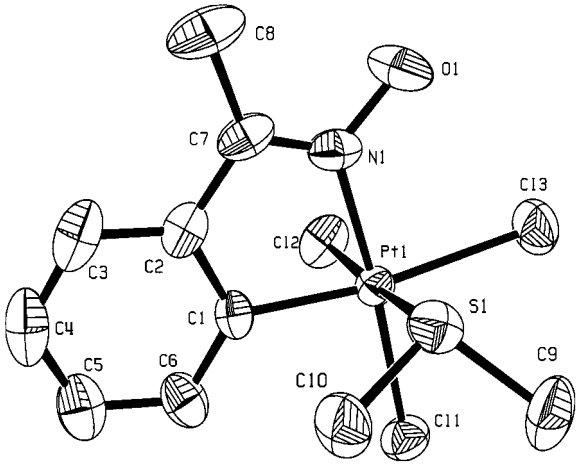

Figure 6. Crystal structure of complex **2a**.

Table 5. Bond Distances (in Å) and Bond Angles (in Degrees) for Complex **2a**[a]

Pt1-Cl1	2.306(2)	N1−C7	1.275(9)
Pt1−Cl2	2.330(2)	C1−C2	1.41(1)
Pt1−Cl3	2.444(2)	C1−C6	1.37(1)
Pt1−S1	2.336(2)	C2−C7	1.46(1)
Pt1−N1	2.019(6)	C2−C3	1.409(9)
Pt1−C1	2.017(5)	C3−C4	1.40(1)
S1−C9	1.807(9)	C4−C5	1.39(1)
S1−C10	1.788(8)	C5−C6	1.40(1)
O1−N1	1.385(7)	C7−C8	1.51(1)
Cl1−Pt1−Cl2	91.64(8)	Cl1−Pt1−Cl3	93.82(7)
Cl1−Pt1−S1	92.44(8)	C1−C2−C7	117.0(5)
Cl1−Pt1−N1	174.6(2)	Cl1−Pt1−C1	94.7(2)
Pt1−C1−C2	111.1(4)	Cl2−Pt1−Cl3	91.60(8)
C3−C2−C7	123.9(7)	Cl2−Pt1−S1	175.90(8)
Cl2−Pt1−N1	89.5(2)	Pt1−C1−C6	127.5(5)
Cl2−Pt1−C1	87.3(2)	Cl3−Pt1−S1	87.73(7)
Cl3−Pt1−N1	91.4(2)	Cl3−Pt1−C1	171.4(2)
C2−C1−C6	121.4(6)	S1−Pt1−N1	86.4(2)
C2−C3−C4	118.9(8)	S1−Pt1−C1	92.7(2)
N1−Pt1−C1	80.1(2)	Pt1−S1−C9	108.0(4)
Pt1−S1−C10	108.4(3)	C9−S1−C10	99.3(4)
C6−C1−C7	153.5(5)	C3−C4−C5	121.1(7)
Pt1−N1−O1	121.7(4)	Pt1−N1−C7	119.0(5)
O1−N1−C7	119.3(6)	C1−C2−C3	119.1(7)
N1−C7−C8	123.1(6)	C4−C5−C6	120.1(8)
C2−C7−C8	124.3(6)	C1−C6−C5	119.4(8)
N1−C7−C2	112.7(7)		

[a] Numbers in parentheses are estimated standard deviations in the least significant digits.

noting that the Pt−H coupling constants for the S−CH_3 resonances differ significantly in complexes **1** and **2** (cf. with J_{PtH} = 24 Hz in **1a**). The ^{1}H NMR spectral data for other ring-substituted complexes **1b**−**e** are also tabulated (Table 4).

The crystal structure of Pt(IV) complex **2a** is shown in Figure 6, whereas bond lengths and bond angles are collected in Table 5. The chloro ligands are facially arranged, the Pt−Cl bond distances being 2.306(2), 2.330(2), and 2.444(2) Å for chloride

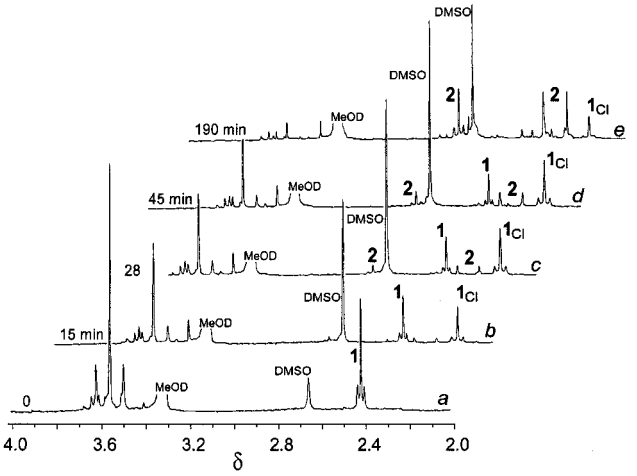

Figure 7. ^{1}H NMR spectral changes of complex **1a** with time observed in the presence of 0.25 M DCl at 64 °C in methanol-d_4.

trans to N, S, and C, respectively, similar to those in **2g**.[11] The bond distances match the ground-state trans influence which increases in the series N < S < C.[21] Other structural features of **2a** are similar to those of **2g** and related Pt(IV) complexes which were discussed in detail previously (see ref 11 and references cited therein). The X-ray crystal structure of the relevant Pt(IV) complex *trans*-(*S*,*N*)-[Pt($OC_6H_2Cl_2CH$═NOH)-$Cl_3(Me_2SO)$] has recently been published by Kukushkin et al.[38] Its Pt−S and Pt−N bond distances of 2.301 and 2.036 Å, respectively, are comparable with those in **2a**, but the ligand arrangement is different. The Pt(IV) sulfoxide compound adopts the meridional coordination of chloro ligands.

^{1}H NMR and UV−Vis Studies of Conversion of 1 into 2. When DCl is added instead of LiCl to the solution of **1a** in methanol-d_4, the ^{1}H NMR spectra of **1a** are similar at the early stages in both cases (cf. Figures 1 and 7b,c). After 15 min, the substitution of chloride for DMSO is noticeable due to the singlet at δ 2.19. Product **2a** shows up after 15−30 min, as suggested by three new resonances at δ 2.24, 2.35, and 2.74 (Figure 7b,c) from two diastereotopic S−CH_3 and C−CH_3 methyls, respectively. The spectra recorded after 45 and 190 min demonstrate that the Pt(II) species transform into **2a**, which dominates after 3 h. The integration allows us to follow the concentration of each species in solution. The concentration profiles in Figure 8 deserve comment. First, the amount of **1a** decreases gradually as evidenced by the signals from the coordinated DMSO and the methyl group of the orthoplatinated aryl oxime. Second, the $\mathbf{1a}_{Cl}$ profile exhibits a maximum at the same point on the time scale as the inflection point at the **2a** profile. Thus, complex $\mathbf{1a}_{Cl}$ is a conceivable precursor of **2**. It

(38) Kukushkin, Y. N.; Krylov, V. K.; Kaplan, S. F.; Calligaris, M.; Zangrando, E.; Pombeiro, A. J. L.; Kukushkin, V. Y. *Inorg. Chim. Acta* **1999**, *285*, 116−121.

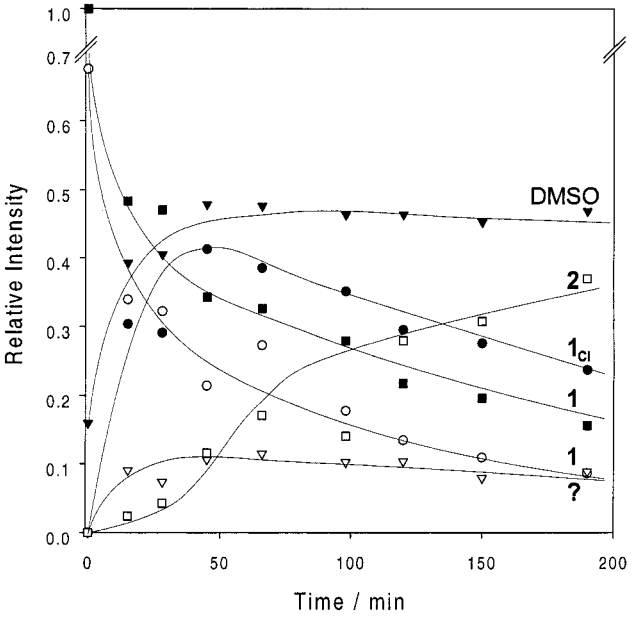

Figure 8. Concentration profiles obtained from the data analogous to those shown in Figure 7 for various species formed during the conversion of **1a** into **2a**. Profiles for **1a** (■ and ○) are obtained from resonances from coordinated DMSO and C−CH_3 (δ 2.44), respectively; profile for $\mathbf{1a}_{Cl}$ (□) is an average from resonances from two diastereotopic S−CH_3 groups and C−CH_3 group; 0.25 M DCl at 64 °C in methanol-d_4.

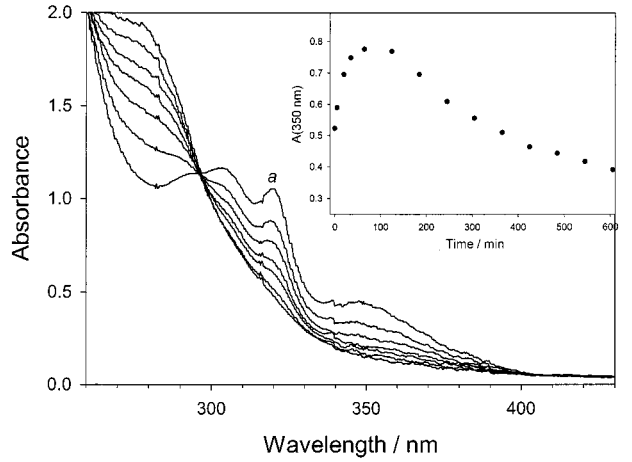

Figure 9. Spectral changes of complex **1a** (0.00025 M) with time in the presence of 0.03 M HCl and 0.1 M $NaClO_4$ at 60 °C in MeOH. Spectrum a was recorded at time $t = 0$ after addition of HCl; other spectra were obtained at $t = 5$, 10, 15, 20, 30, and 50 min, respectively. (Inset) Biphasic nature of the deoxygenation, shown by following the absorbance change at 350 nm at 0.008 M HCl and 0.094 M $NaClO_4$ at 60 °C in MeOH.

is worth noting that the inset in Figure 9 matches the concentration profile for $\mathbf{1a}_{Cl}$ in Figure 8, and this provides extra evidence for $\mathbf{1}_{Cl}$ as the key intermediate. Third, the concentration of free DMSO is practically constant over the course of the experiment. The same run carried out at 0.1 M $NaClO_4$ showed a 2-fold rate increase.

The conversion of **1a** into **2a** can be clearly observed by UV−vis spectroscopy at higher HCl concentrations (Figure 9). The process is characterized by the absorbance decrease at 320 and 350 nm, the isosbestic point being held at 301 nm. There are two species involved, viz., $\mathbf{1a}_{Cl}$ and **2a**, since the final spectrum corresponds to that of **2a** under the identical conditions.[39] The

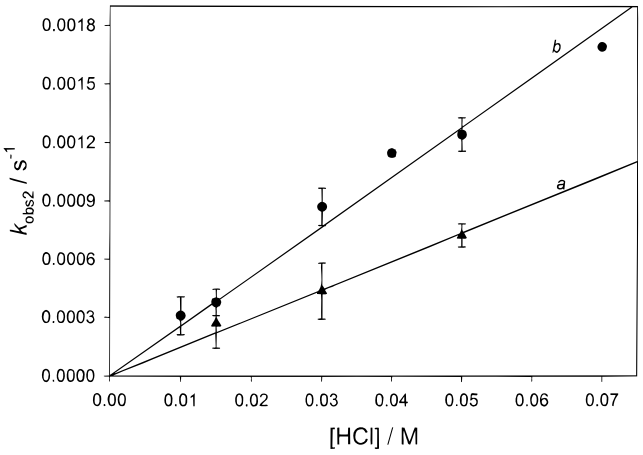

Figure 10. Pseudo-first-order rate constants k_{obs2} for the second phase as a function of HCl concentration for conversion of complex **1a** into **2a** in the absence (a) and in the presence of 0.1 M $NaClO_4$ (b) at 55 °C in methanol solvent.

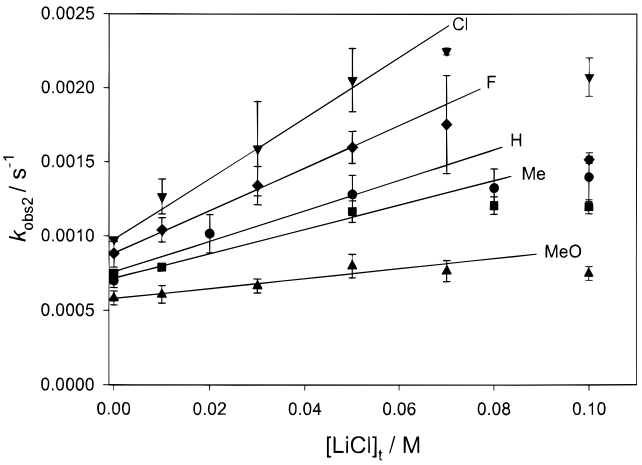

Figure 11. Pseudo-first-order rate constants k_{obs2} for the second phase as a function of LiCl concentration for conversion of complexes **1** into **2**; 0.03 M HCl, 0.1 M $NaClO_4$, 55 °C, methanol solvent.

absorbance variation at 350 nm (inset to Figure 9) at lower [HCl] (0.008 M) confirms the biphasic conversion of **1** into **2**.

Kinetics of Formation of Complexes 2. At [HCl] > 0.008 M, the first phase proceeds rather fast when followed by conventional spectrophotometry, and the buildup in absorbance at 350 nm does not occur. Thus, the kinetics of the second phase can directly be measured. The largest absorbance change for **1a** is observed at 320 nm, and this wavelength was chosen for collecting kinetic data. The pseudo-first-order rate constants k_{obs2} were evaluated at 55 °C as functions of HCl, LiCl, and $NaClO_4$ concentrations. Pronounced acid catalysis emphasizes the second phase. Figure 10 shows the k_{obs2} versus [HCl] plot with and without 0.1 M $NaClO_4$. There is a first-order dependence in HCl, and $NaClO_4$ accelerates the reaction. The slopes of the linear plots equal $(2.56 \pm 0.09) \times 10^{-2}$ and $(1.47 \pm 0.06) \times 10^{-2}$ M^{-1} s^{-1} with and without $NaClO_4$, respectively, the ratio being 1.74, in agreement with the ^1H NMR data.

Plots of k_{obs2} as a function of [LiCl] are shown in Figure 11. At [LiCl] < 0.06 M, the plots match those obtained for k_{obs1} (cf. data for **1a** in Figure 4). Since the second phase does not occur at [HCl] = 0 and k_{obs2} is independent of the concentration of added DMSO (0.0028−0.012 M), rate law at [LiCl] < 0.06

(39) This is important, since the spectrum of **2a** in MeOH was found to be dependent on concentration of HCl (see Figures 4S and 5S of the Supporting Information).

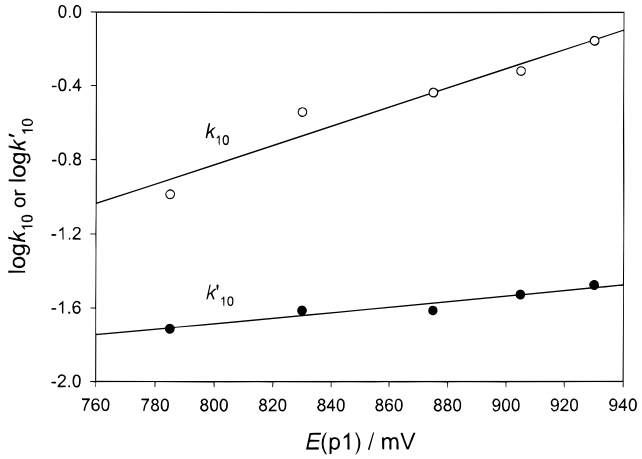

Figure 12. Dependencies of log k_{10} (○) and log k_{10}' (●) (eq 10) on $E(p1)$ for the formation of **2** at 55 °C in methanol solvent.

M is given by eq 10. The corresponding numerical values k_{10}'

$$k_{obs2}[H^+]^{-1} = (k_{10}' + k_{10}[LiCl]) \quad (10)$$

and k_{10} for complexes **1a**−**e** are placed in Table 3. The kinetic data in Figure 11 show, however, that at [LiCl] > 0.06 M, the k_{obs2} values level off as the concentration of LiCl increases, indicating that eq 11 may hold. The data in Figure 11 were

$$k_{obs2}[H^+]^{-1} = \frac{a + b[LiCl]}{c + [LiCl]} \quad (11)$$

fitted to eq 11, and the values of *a*, *b*, and *c* are summarized in Table 1S (Supporting Information). Moreover, rate retardation by LiCl is observed for electron-poor complexes **1d**,**e** when the concentration of LiCl approaches 0.1 M.

The effect of substituents on k_{10}' and k_{10} is shown in Figure 12, where log k_{10} and log k_{10}' are plotted against $E(p1)$. The LiCl-dependent pathway is again more sensitive to the electronic effects and the slopes equal (1.50 ± 0.25) and (5.2 ± 0.8) V^{-1} for the k_{10}' and k_{10} pathways, respectively. When log *b* was plotted against $E(p1)$, the slope was 5.1 ± 0.9 V^{-1}; i.e., there is a clear parallel between the kinetic parameters k_{10} and *b*.

Discussion

General Comments and Stoichiometric Mechanism. Spectral, electrochemical, and kinetic data obtained in this work emphasize a nonconcerted mechanism of reaction 4. The particular fragments of complex **1** which undergo transformation, viz., coordinated DMSO and the Pt(II) center, are insufficiently tuned for the redox reaction, and, therefore, several preliminary steps are required to adjust their reactivity. In particular, neutral Pt(II) complexes **1** must be converted into the easier-to-oxidize anionic species $\mathbf{1}_{Cl}$ in reaction 5, in which the orthoplatinated ligand plays a key role. It is well documented that DMSO is easily substituted by chloride in Pt(II) complexes when activated by an appropriate ligand located cis to it.[40,41] It is thus the σ-bound phenyl ring of the orthoplatinated oxime that is a perfect cis-labilizing ligand.

It is equilibrium 5 that (i) generates the reactive species, viz., $\mathbf{1}_{Cl}$ and unbound DMSO, which is easier to protonate in a free form;[42] (ii) separates the reacting fragments, ruling out an *intramolecular* mechanism; (iii) adjusts them for the subsequent redox transformation; and (iv) forces the reaction to proceed intermolecularly. Rate expression 10 indicates that a proton is included in the transition state and either DMSO (mechanism 1, MI) or complex $\mathbf{1}_{Cl}$ (mechanism 2, MII) can be protonated. The simplest stoichiometric mechanism of the reaction with a proton ambiguity is given by eqs 12−16. Here, eq 13 shows

MI		MII		
$Me_2S{=}OH^+ \rightleftharpoons Me_2S{=}O + H^+$	or	$\mathbf{6} \rightleftharpoons \mathbf{1}_{Cl} + H^+$	K_a	(12)
$\mathbf{1} \rightleftharpoons \mathbf{1}_{Cl}$			k_s, k_{-s}	(13)
$\mathbf{1} + Cl^- \rightleftharpoons \mathbf{1}_{Cl} + Me_2S{=}O$			k_{Cl}, k_{-Cl}	(14)
$\mathbf{1}_{Cl} + Me_2S{=}OH^+ \rightarrow [Pt^{III}{-}O(H){-}SMe_2]$	or	$\mathbf{6} + Me_2S{=}OH \rightarrow [Pt{-}SMe_2{-}OH]$	k_{15}	(15)
$[Pt^{III}{-}O(H){-}SMe_2] \rightarrow \mathbf{2}$	or	$[Pt{-}SMe_2{-}OH] \rightarrow \mathbf{2}$	fast	(16)

schematically substitution of DMSO by chloride via the solvent-dependent pathway; eq 15 is the rate-limiting step, the nature of which is specified below; and eq 16 is the fast step, leading to **2**. Applying the steady-state approximation with respect to $\mathbf{1}_{Cl}$ and taking into account the mass balance equation $[Pt]_t = [\mathbf{1}] + [\mathbf{1}_{Cl}]$, eqs 12−16 lead to expression 17 for k_{obs2} in terms of MI. Here, $[Cl^-]_t$ and $[Me_2SO]_t$ denote total concentrations

$$k_{obs2} = \frac{(k_s + k_{Cl}[Cl^-]_t)k_{15}K_a^{-1}[Me_2SO]_t[H^+]}{k_s + k_{-s} + k_{Cl}[Cl^-]_t + (k_{-Cl} + k_{15}[H^+]/K_a)[Me_2SO]_t} \quad (17)$$

of chloride and DMSO, respectively. Since in the concentration range studied the reaction is strictly first-order in $[H^+]$, eq 17 should be rewritten as eq 18 on the assumption that $k_{-Cl} \gg k_{15}[H^+]/K_a$, which seems to be valid since the basicity of DMSO is low. The rate expression 18 is in agreement with the observed

$$k_{obs2} = \frac{(k_s + k_{Cl}[Cl^-]_t)k_{15}K_a^{-1}[Me_2SO]_t[H^+]}{k_s + k_{-s} + k_{Cl}[Cl^-]_t + k_{-Cl}[Me_2SO]_t} \quad (18)$$

dependencies of k_{obs2} on the concentrations of added chloride and DMSO. One arrives directly at eq 18 in terms of MII on the assumption that the concentration of **6** is much lower than those of **1** and $\mathbf{1}_{Cl}$. As emphasized above, the reaction rate is essentially independent of $[Me_2SO]_t$, and in terms of eq 18 this suggests that at low chloride concentrations $(k_s + k_{-s} + k_{Cl}[Cl^-]_t) \ll k_{-Cl}[Me_2SO]_t$, providing further simplification:

$$k_{obs2} = (k_s + k_{Cl}[Cl^-]_t)k_{15}(k_{-Cl}K_a)^{-1}[H^+] \quad (19)$$

Thus, the dependence of k_{obs2} on $[Cl^-]_t$ at low LiCl concentrations should be linear with a positive intercept (eq 19), and the data in Figure 11 demonstrate that this is the case. However, when the relation $(k_s + k_{-s} + k_{Cl}[Cl^-]_t) \ll k_{-Cl}[Me_2SO]_t$ does not hold, k_{obs2} should level off as the chloride concentration becomes higher (eq 18). The experimental evidence for this is found in Figure 11 and eq 11. Thus, the stoichiometric mechanisms MI and MII are in accord with the experimental kinetic data. The rate law 10 corresponds to eq 19 derived from eqs 12−16. The rate constants k_{10}' and k_{10} in eq 10 must be associated with $k_s k_{15}/k_{-Cl}K_a$ and $k_{Cl}k_{15}/k_{-Cl}K_a$ (eq 19), respectively.

(40) Lanza, S.; Minniti, D.; Romeo, R.; Tobe, M. *Inorg. Chem.* **1983**, *22*, 2006−2010.

(41) Romeo, R.; Nastasi, N.; Scolaro, L. M.; Plutino, M. R.; Albinati, A.; Macchioini, A. *Inorg. Chem.* **1998**, *37*, 5460−5466.

(42) The reversible protonation of DMSO in MeOH is observed by UV−vis spectroscopy at 202 nm. The estimated value of pK_a is around 0. The data are shown in Figure 6S.

Intimate Mechanistic Features: Substitution of DMSO in Complexes 1. The mechanism of substitution of DMSO in Pt(II) complexes by various ligands was intensively studied during past three decades (see ref 43 and the literature cited therein). Efforts were aimed at differentiation between associative and dissociative substitution mechanisms.[18−20] In this work, the previous knowledge is used for assigning mechanistic steps prior to reduction of DMSO. The orthoplatinated ligand in **1** affects the rate law and contributions of the solvent- and chloride-driven pathways into the overall rate. In fact, the substitution of DMSO by chloride in complexes $[Pt(en)(DMSO)_2]^{2+}$ [40] and $[PtMe(LL)(DMSO)]^+$ (LL = bis-2-pyridylamine)[41] in MeOH follows the first-order kinetics in chloride without intercept, showing the insignificance of the solvolitic pathway. In contrast, the latter dominates for complexes **1**. The k_{Cl} pathway is unambiguous for electron-poor complexes and negligible for MeO- and Me-substituted molecules **1b**,**c**. This trend is also seen in Figure 5, and the log k_{Cl}, not log k_s, versus $E(p1)$ plot has a meaningful positive slope. As mentioned above, different sensitivity of k_s and k_{Cl} to electronic characteristics of **1** is due to different charges of methanol and chloride. Negatively charged chloride is obviously more sensitive to the redox potential of the target complex. The kinetic behavior of **1** resembles that of complexes *trans*-$[Pt(aryl)Cl(SMe_2)_2]$, the rate of substitution at which is also independent of the concentration of such nucleophiles as Br^- and N_3^-.[44]

The activation enthalpy of 24.5 kJ mol^{-1} for the k_s pathway for **1a** is too low to mirror the rate-limiting dissociative Pt−Cl bond cleavage, and the associative mechanism must be operative. In accord with this is the $\Delta S^{\ddagger}$ of −81 J K^{-1} mol^{-1}, typical of a bimolecular reaction with the entropy loss in the transition state. The same mechanism is valid for the k_{Cl} pathway, since the electron-deficient complexes **1** react faster. Thus, the mechanistic information on reaction 5 supports previous conclusions[14,15] that σ-bound orthoplatinated ligands, although possessing strong ground-state trans influence and speeding up substitution and bridge splitting, do not bring about the associative → dissociative mechanistic changeover.

Intimate Mechanistic Features: Deoxygenation of DMSO. The intriguing question here is why the reaction does not occur intramolecularly within **1**, but rather intermolecular activation, at first glance less favorable, is preferred. The necessity of redox tuning of the Pt(II) species has already been emphasized. It should also be taken into account that, in addition to electron transfer, the reduction of DMSO involves S=O bond cleavage. The binding of Pt(II) with DMSO could, in principle, elongate the S=O bond and thus favor the reaction. However, thorough analysis of the structural data[3] has led to the conclusion that the coordination of DMSO with Pt(II) via sulfur shortens the S=O bond in the ground state. The average bond distances in free and S-bound DMSO are 1.492 and 1.471 Å, respectively. The bond length increases when DMSO is bound to Pt(II) via oxygen (1.540 Å),[3] but the largest elongation (1.585 Å) occurs on protonation of the sulfoxide oxygen. Thus, DMSO dissociates from **1** to generate a species with a weaker sulfur−oxygen bond. It was not, therefore, surprising to observe the acid catalysis with plausibly protonated DMSO as a reactive species in terms of MI (Scheme 1). Further elongation of the S=O bond is feasible in the Pt−O-bonded intermediate **4**, with the weakest sulfur−oxygen bond due to both protonation and O-coordination. The rate-limiting first electron transfer affords the Pt(III)

Scheme 1

MI

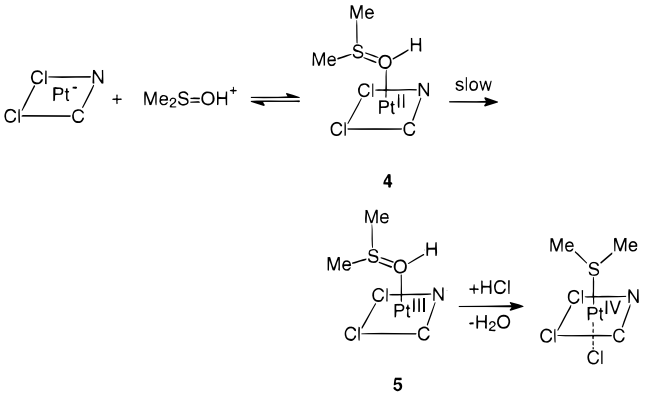

Scheme 2

MII

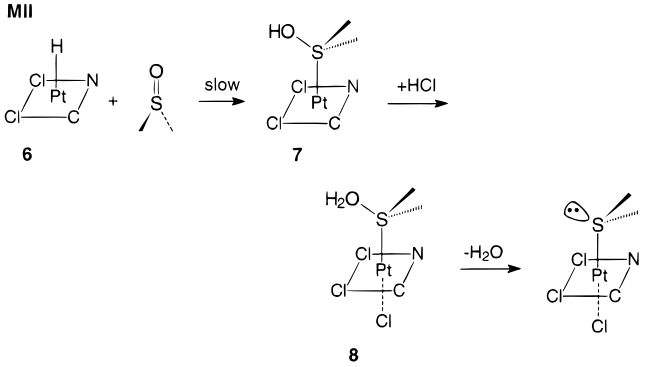

intermediate **5** with a weakened sulfur−oxygen bond. The second electron transfer, to give Pt(IV), leads to S−O bond cleavage, and the oxygen dissociates as water in the presence of HCl. Five-coordinated species are not unusual and are well documented[45−48] not only as intermediates.[49] A square-pyramidal geometry of **4** as shown in Scheme 1 is one of the possibilities. The orthometalated C,N-chelate, which is a π-acceptor due to the σ-bound aryl ring, and two chloro ligands are capable of creating a trigonal-bipyramidal structure, with two chlorides occupying axial positions.[47]

The kinetically indistinguishable mechanism 2 is shown is Scheme 2. It involves the protonation of the Pt(II) center to afford the platinum(II)−proton or platinum(IV)−hydride moiety followed by the rate-limiting insertion of the S=O double bond into the Pt−H bond of intermediate **6**. Hydride complexes of Pt(IV) are now widely invoked to rationalize mechanisms of catalytic reactions.[12,50] Their existence has been confirmed previously[51−54] and in this work by the example of protonation of complex **1c** (anionic species $\mathbf{1}_{Cl}$ cannot be generated in the absence of DMSO, see above). A five-coordinate hydride Pt(IV) intermediate similar to **6** has recently been proved to exist in the elimination reaction of methane from $[Pt(H)Me_2(L)]^+$ (L = bis(2-pyridylmethyl)amine).[55] The rate-limiting step, which

(43) Romeo, R.; Scolaro, L. M.; Nastasi, N.; Mann, B. E.; Bruno, G.; Nicolo, F. *Inorg. Chem.* **1996**, *35*, 7691−7698.

(44) Wendt, O. F.; Oskarsson, Å.; Leipoldt, J. G.; Elding, L.-I. *Inorg. Chem.* **1997**, *36*, 4514−4519.

(45) Wehman-Ooyevaar, I. C. M.; Grove, D. M.; de Vaal, P.; Dedieu, A.; van Koten, G. *Inorg. Chem.* **1992**, *31*, 5484−5493.

(46) Fanizzi, F. P.; Intini, F. P.; Maresca, L.; Natile, G.; Lanfranchi, M.; Tiripicchio, A. *J. Chem. Soc., Dalton Trans.* **1991**, 1007−1015.

(47) Fanizzi, F. P.; Maresca, L.; Natile, G.; Lanfranchi, M.; Tiripicchio, A.; Pacchioni, G. *J. Chem. Soc., Chem. Commun.* **1992**, 333−335.

(48) Albano, V. G.; Natile, G.; Panunzi, A. *Coord. Chem. Rev.* **1994**, *133*, 67−114.

(49) Otto, S. Structure and Reactivity Relationships in Platinum(II) and Rhodium(I) Complexes. Ph.D. Thesis, University of the Free State, Bloemfontein, South Africa, 1999.

(50) Rendina, L. M.; Puddephatt, R. J. *Chem. Rev.* **1997**, *97*, 1735−1754.

affords **7**, is analogous to insertion of carbon−carbon double bonds into the M−H bonds of transition metal complexes. Subsequent protonation of the *S*-hydroxyl generates a good leaving group, and the water departure accomplishes MII. To our knowledge, the insertion of the S═O bond into the metal−hydride one has never been proposed to account for the mechanism of reaction of type 1. However, it seems to be due to the acid catalysis. Key steps of MII match those for related processes such as platinum-catalyzed hydrogenation and hydrosilylation of alkenes.[56,57] Scheme 2 fits also the biphasic nature of the process, since the first step is needed to generate $\mathbf{1}_{Cl}$ and free DMSO. Anionic complex $\mathbf{1}_{Cl}$ must be more susceptible to protonation than its neutral precursor **1**.

The rate retardation at high LiCl concentrations is readily accountable in terms of both MI and MII, since the formation of **4** or **6** is disfavored when the fifth coordination site is occupied by the chloro ligand. Five-coordinated species of the type $[PtI_2(PR_3)_3]I$ generated by attack of halides at square-planar Pt(II) complexes have recently been isolated and characterized by a single-crystal X-ray study.[49]

Electron-poor complexes **1** react faster (Figure 12). This observation is controversial, since they are more difficult to oxidize. The discrepancy is also rationalizable in terms of MI and MII. In fact, several phenomena contribute to the overall rate, i.e., generation of $\mathbf{1}_{Cl}$ and its subsequent transformations into **4** and **5** (MI) or **6** and **7** (MII). The formation of $\mathbf{1}_{Cl}$ and the following steps should have opposite sensitivity to the electronic effects. The electron-deficient species have higher affinity to chloride, and their corresponding rate constants k_{Cl} differ by a factor of 6 in the series (Table 3). On the condition that this process contributes most into the electronic effects in formation of **2** ($k_{10} = k_{Cl}k_{15}[H^+]/k_{-Cl}K_a$), the tendency observed is easy to understand.

Theoretical Modeling. A Density Functional Study. Discrimination between MI and MII is difficult on the basis of exclusively kinetic data. Therefore, an attempt was made to probe the mechanisms by the quantum-chemical analysis using density functional theory (DFT), which proved to be useful for theoretical treatments of transition metal complexes. First, the orbital analysis has been performed with a goal of seeing any orbital advantage for the interaction between the elucidated reactive species, viz., $\mathbf{1}_{Cl}$/$DMSOH^+$ (MI) and **6**/DMSO (MII). A LUMO/HOMO diagram for the species indicated is shown in Figure 13. It should first be mentioned that the DFT results in Figure 13 support the conclusions derived from the electrochemical data in Table 2. The HOMO of $\mathbf{1}_{Cl}$ is higher than that of **1**, accounting for the easier oxidation of the anionic complexes. As far as the mechanistic discrimination is concerned, the data in Figure 13 suggest that MII involving **6** and free DMSO is better. Comparison of the $\mathbf{1}_{Cl}$ + $DMSOH^+$ and **6** + DMSO pairs of reactants indicated that the gap between $\mathbf{1}_{Cl}$ HOMO and $DMSOH^+$ LUMO (0.1918 au) is much bigger than the gap between DMSO HOMO and **6** LUMO (0.0930 au). However, there is inverse order of MO's in the two schemes. But this most likely does not play a crucial role, since it is already Pt(IV) in complex **6**.

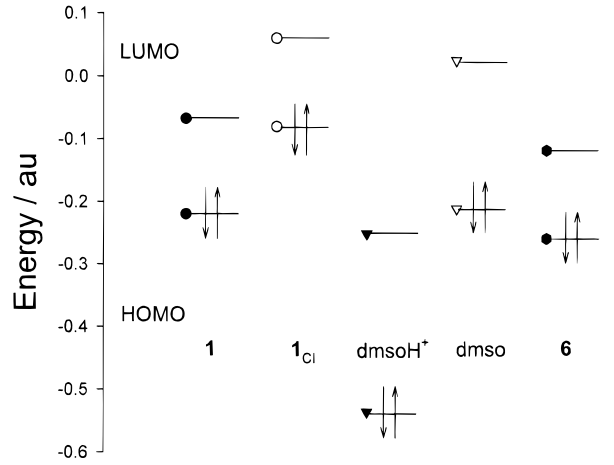

Figure 13. Calculated molecular orbital diagram of species involved in mechanisms MI and MII (au = atomic units).

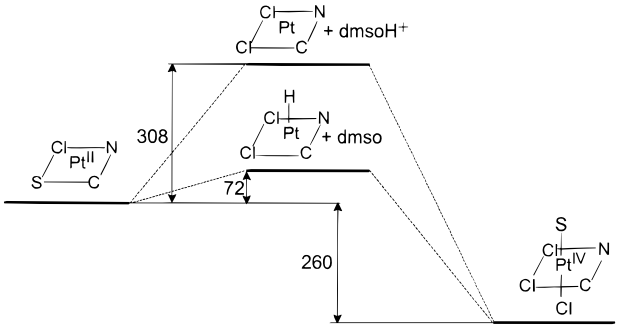

Figure 14. Calculated B3LYP energy profiles for MI and MII showing that MII requires less energy. Numbers show energy in kilojoules per mole.

Results of comparative analysis of energies of conceivable intermediates in MI and MII, viz., $\mathbf{1}_{Cl}$/$DMSOH^+$ and **6**/DMSO, are presented in Figure 14. These are in accord with conclusions derived from the MO energies. The MII pathway demands much less energy for generation of the **6**/DMSO pair of intermediates compared to $\mathbf{1}_{Cl}$/$DMSOH^+$ considering complex **1** and HCl as the initial state. The energy difference (236 kJ mol^{-1}) is striking, and although the energies of intermediates, in contrast to the transition state energies, do not provide straightforward information about the activation barriers, one may state with confidence that the MII mechanism is definitely energetically preferred. This conclusion is somewhat surprising since it is still more customary to treat nonmetal atoms as better bases compared to transition metal ions.

A question which deserves comment is how the system copes with the unfavorable thermodynamics mentioned in the Introduction. The DFT study suggests an energy gain in 260 kJ mol^{-1}. It is presumably due to the favorable binding of Me_2S to Pt(IV), since the sulfides are better ligands for Pt(II) and Pt(IV) compared to sulfoxides. Therefore, the formation of a new Pt−S bond makes the entire process 1 thermodynamically favorable. It should also be added that the Pt(II) → Pt(IV) oxidative transitions induced by mild oxidants have been documented. The most unexpected and striking is the oxidation by water of electron-rich Pt(II) complexes exemplified by the exciting works from the Canty group.[12,53,58] It has recently been shown that even *cis*-$[PtCl_2(SOMe_2)_2]$ is oxidized by dioxygen under certain conditions.[59]

(51) Hill, G. S.; Vittal, J. J.; Puddephatt, R. J. *Organometallics* **1997**, *16*, 1209−1217.
(52) Jenkins, H. A.; Yap, G. P. A.; Puddephatt, R. J. *Organometallics* **1997**, *16*, 1946−1955.
(53) Canty, A. J.; Fritsche, S. D.; Jin, H.; Patel, J.; Skelton, B. W.; White, A. H. *Organometallics* **1997**, *16*, 2175−2182.
(54) Prokopchuk, E. M.; Jenkins, H. A.; Puddephatt, R. J. *Organometallics* **1999**, *18*, 2861−2866.
(55) Fekl, U.; Zahl, A.; van Eldik, R. *Organometallics* **1999**, *18*, 4156−4164.
(56) Kwiatek, J. In *Hydrogenation and Dehydrogenation*; Schrauzer, G. N., Ed.; Marcel Dekker: New York, 1971; pp 13−57.
(57) Creve, S.; Oevering, H.; Coussens, B. B. *Organometallics* **1999**, *18*, 1967−1978.

Biomimetic Relevance of the Reaction. There is an analogy between the Pt(II)-promoted deoxygenation reported here and the enzymatic reaction catalyzed by the Mo-dependent DMSO reductase.[60,61] The stoichiometry of the enzymatic process (eq 20) parallels eq 1. The enzymatic reduction is a multistep process

$$\text{enzyme}{-}\text{Mo(IV)} + \text{Me}_2\text{S}{=}\text{O} + 2\text{H}^+ \rightarrow \text{enzyme}{-}\text{Mo(VI)} + \text{Me}_2\text{S} + \text{H}_2\text{O} \quad (20)$$

involving two, one-electron steps. At pH 8.5, two oxidations for *Rhodobacter sphaeroides* DMSO reductase observed at +37 and +83 mV (versus NHE) are associated with the Mo(IV/V) and Mo(V/VI) redox transitions, respectively,[61] which, of course, occur more cathodically compared to the Pt(II) mimetic reported here. According to the present state of knowledge, DMSO is coordinated with Mo via oxygen in the key enzymatic intermediate. A proton is also believed to play an important role in the enzymatic system.[60] In general, the mechanism of the bioreaction matches better the MI mechanism which seems, however, less probable than MII in light of the DFT study. Thus, there is a similar pathway in the unnatural Pt(II) system, although the soft sulfur center of DMSO is more useful for binding with a soft Pt(II) center compared to hard oxygen. The acid catalysis is a key feature in the platinum(II)-promoted reaction. These analogies make it possible to view the platinum system reported in this work as a true functioning mimetic of the Mo-dependent dimethyl sulfoxide reductase.

Conclusion. The system described represents an interesting mechanistic example in which the intuitively *intramolecular* conversion of **1** into **2** does not occur as such because the participating fragments of the starting complex **1** are insufficiently tuned to undergo deoxygenation of DMSO coupled with the oxidation of Pt(II) into Pt(IV). The system adopts, at first glance, a less advantageous *intermolecular* pathway which makes it possible to adjust independently the reactivities of the two participating species. A novel mechanism of deoxygenation is proposed involving the insertion of the sulfoxide S=O bond into the platinum−hydride moiety formed on protonation of the anionic intermediate $\mathbf{1}_{\text{Cl}}$.

Experimental Section

Methods. Spectrophotometric and kinetic measurements were carried out on a Shimadzu UV-160A spectrophotometer equipped with a CPS-240A cell positioner/temperature controller or a Hitachi 150-20 instrument with a thermostated by circulating water cell compartment. ^{1}H NMR spectra were recorded on CXP-200 Bruker and Varian UNITY 300 instruments with a residual solvent signal as internal standard. Electrochemical measurements were made in a three-electrode cell with a pyrolitic graphite working electrode at 25 and 55 °C. A potential sweep was generated with an IPC-3 instrument interfaced with a personal computer. The working electrode was polished with a diamond paste before every new measurement. Unless otherwise indicated, potentials are versus saturated calomel electrode (SCE) throughout.

Reagents. *cis*-$[PtCl_2(SOMe_2)_2]$ was obtained according to the procedure of Price et al.[62] Ring-substituted acetophenones 4-RC_6H_4-COMe (R = H, MeO, Me, F, and Cl) were purchased from Lancaster and then converted into corresponding oximes 4-$RC_6H_4C(Me){=}NOH$ by the action of hydroxylamine according to the classical procedure.[63] Complexes **1** were prepared from the oximes and *cis*-$[PtCl_2(SOMe_2)_2]$ in refluxing methanol as described previously.[11] Methanol of the highest purity (Khimed), used as a reaction medium, was utilized as received. Other reagents used in this work were of the highest quality available.

Synthesis of Complex 1f. A 18.2 g (0.126 mol) portion of octanoic acid (Reakhim) was refluxed with $SOCl_2$ (22.5 g, 0.189 mol) for 2 h, and then acid chloride formed was distilled in a vacuum (82 °C, 16 mmHg). Yield 85%. Subsequent Friedel−Crafts acylation of benzene (30 mL) in the presence of $AlCl_3$ (6.7 g, 0.05 mol) by octanoic acid chloride (8.1 g, 0.05 mol) for 4 h at ambient temperature as described elsewhere[64] afforded phenyl *n*-heptyl ketone (80%). The latter was converted into phenyl *n*-heptyl ketone oxime (85%) by reaction with hydroxylamine hydrochloride.[63] ^{1}H NMR ($CDCl_3$): δ 0.87 (t, 3H, CH_3), 1.26 (m, 8H), 1.49 (m, 2H, NCH_2CH_2), 2.80 (t, 2H, NCH_2), 7.34−7.41 (m, 3H, Ar), 7.57−7.63 (m, 2H, Ar), 8.62 (bs, 1H, OH). *n*-Heptyl ketone oxime (0.0508 g, 0.23 mmol) and *cis*-$[PtCl_2(SOMe_2)_2]$ (0.1 g, 0.23 mmol) in 20 mL of MeOH were refluxed for 12 h, and the solvent was then evaporated to dryness. The residue was separated by TLC using Silufol plates and benzene−ethyl acetate (15:1) as eluent. The first band was separated to yield **1f** (35%). Anal. Calcd for $C_{16}H_{26}ClNO_2PtS$: C, 37.5; H, 5.0. Found: C, 36.9; H, 5.1. ^{1}H NMR ($CDCl_3$): δ 0.89 (t, 3H, CH_3), 1.28 (m, 8H), 1.65 (m, 2H, NCH_2CH_2), 2.79 (t, 2H, NCH_2), 3.54 (s, 6H, J_{PtH} = 24 Hz, SCH_3), 7.15 (m, 4H, Ar), 8.04 (dd, 1H, J_{PtH} = 52 Hz, H6), 10.11 (s, 1H, OH).

Synthesis of Complexes 2 (by the Example of 2a). Complex **1a** (0.0394 g, 0.089 mmol) was dissolved in 6 mL of methanol, and then 28 μL of concentrated HCl was introduced. The mixture was refluxed for 5 h and then cooled. Yellow crystals precipitated were separated, washed with cold methanol, and air-dried. Yield 67.2% (0.033 g). Anal. Calcd for $C_{10}H_{14}Cl_3NOPtS$: C, 24.13; H, 2.84; Pt, 39.19. Found: C, 24.25; H, 2.64; Pt, 39.60. Exactly the same procedure was employed for the preparation of other complexes **2**; yields and their characteristics are summarized in Table 4. Satisfactory analytical data (C, H, N, and Cl) were obtained for complexes **1b**−**e**.

Synthesis of Complex *trans*-(*N*,*N*)-[Pt^{II}(C_6H_4-2-CMe=NOH)Cl(py)] (3). Compound **3** was obtained by refluxing **1a** (0.0344 g, 0.077 mmol) with pyridine (12 μL, 0.15 mmol) in 6 mL of MeOH for 1.5 h. Dark-yellow crystals that precipitated after cooling of the solution were filtered off, washed with cold methanol, and air-dried. Yield 87%. The ^{1}H NMR spectrum of the material was identical with that of complex **3** which was prepared using another procedure and characterized by an X-ray structural study.[15]

Kinetic Measurements. Stock solutions of complexes **1** (ca. 1.3×10^{-3} M) were prepared in methanol solvent. UV−vis measurements indicated that the spectra of the solutions remained unchanged over several weeks. An aliquot of such a solution (ca. 0.4 mL) was introduced to a 1-cm quartz cuvette, followed by addition of the required amount of LiCl, HCl, or $NaClO_4$ dissolved in MeOH. The total concentration of **1** in the cell was usually around 2.5×10^{-4} M; concentrations of the inorganic additives used are indicated in the legends to the figures throughout the paper. Different wavelengths were chosen for monitoring the first and the second phases of the deoxygenation reaction. The substitution of DMSO by chloride was usually monitored at 353 nm. Since the spectrum of the methoxy-substituted complex **1b** was somewhat different compared with those of other complexes, the wavelength of 327 nm was selected. The kinetics of the second phase was monitored by following a decrease in absorbance of a long-wavelength maximum of the corresponding compound (Table 1). Good first-order kinetic curves were usually obtained for the first and the second phases, and they were quantified by nonlinear least-squares fitting of the absorbance versus time plots to the equation $A = A_\infty + (A_o - A_\infty)\{\exp(-k_{obs}t)\}$, where A, A_∞, and A_o are absorbances at time t, ∞, and $t = 0$, respectively. Satisfactory first-order dependencies were normally observed in a matter of 4−5 half-lives. All calculations were performed using a SigmaPlot 4.0 package.

(58) Canty, A. J.; Honeyman, R. T.; Roberts, A. S.; Traill, P. R.; Colton, R.; Skelton, B. W.; White, A. H. *J. Organomet. Chem.* **1994**, *471*, C8−C10.

(59) Davies, M. S.; Hambley, T. W. *Inorg. Chem.* **1998**, *37*, 5408.

(60) Baugh, P. E.; Garner, C. D.; Charnock, J. M.; Collison, D.; Davies, E. S.; McAlpine, A. S.; Bailey, S.; Lane, I.; Hanson, G. R.; McEwan, A. G. *J. Biol. Inorg. Chem.* **1997**, *2*, 634−643.

(61) George, G. N.; Hilton, J.; Temple, C.; Prince, R. C.; Rajagopalan, K. V. *J. Am. Chem. Soc.* **1999**, *121*, 1256−1266.

(62) Price, J. H.; Williamson, A. N.; Schramm, R. F.; Wayland, B. B. *Inorg. Chem.* **1972**, *11*, 1280−1284.

(63) Beckman, E. *Chem. Ber.* **1890**, *23*, 1680−1692.

(64) *Organikum. Organisch-Chemisches Grundpraktikum*; VEB Deutscher Verlag der Wissenschaften: Berlin, 1976.

Quantum-Chemical Calculations. These were performed using Gaussian 94[65] at the B3LYP level of theory. The basis used for carbon, nitrogen, oxygen, and hydrogen atoms was 6-31G with the polarization functions (6-31G**). For platinum, sulfur, and chlorine the basis used was LANL2DZ[66−68] with pseudopotential. A complete list of calculation results can be found in Table 4S of the Supporting Information.

Crystallography. Data Collection and Structure Determination of 2a. A yellow parallelepiped-shaped crystal was glued on top of a cactus needle and transferred to an Enraf-Nonius CAD4 diffractometer for data collection (graphite-monochromatized Mo Kα radiation). Unit cell dimensions were determined from a least-squares treatment of the setting angles of 24 reflections with $17 < \theta < 19$. The X-ray single-crystal data were corrected for Lorentz, polarization, and absorption effects (empirical correction based on Ψ-scans). The atomic scattering factors were taken from the *International Tables for X-ray Crystallography*.[69] All calculations were performed with the CAD4-SDP program package. The Pt, S, and Cl atoms were found by direct methods, and the remaining non-hydrogen atoms were located from the subsequent Fourier synthesis. Refinement on *F* was carried out by full-matrix least-squares techniques. All non-hydrogen atoms were refined with anisotropic thermal parameters. Hydrogen atoms were not included in the refinement. Additional details of structure determination are given in Table 6.

Acknowledgment. The research described in this publication was made possible in part by financial support from the Russian Foundation for Basic Research (98-03-33023a) and INTAS (97-0166). We thank Irina Panyashkina and Valentina Ryzhova for experimental assistance.

Appendix

According to eq 5, the equilibrium constant K_x is given by eq 1A.

$$K_x = \frac{[\mathbf{1}_{Cl}][DMSO]}{[\mathbf{1}][Cl^-]} \quad (1A)$$

The absorbance is a sum of two terms:

$$A = \epsilon_1[\mathbf{1}] + \epsilon_{Cl}[\mathbf{1}_{Cl}] \quad (2A)$$

Using the mass balance equation ($[Pt]_t = [\mathbf{1}] + [\mathbf{1}_{Cl}]$) and since $[\mathbf{1}_{Cl}] = [DMSO]$, one arrives at eq 3A:

$$K_x = \frac{[\mathbf{1}_{Cl}]^2}{([Pt]_t - [\mathbf{1}_{Cl}])[Cl^-]} \quad (3A)$$

Since $[Cl^-] > [Pt]_t$, the solution of the quadratic equation makes it possible to calculate the equilibrium concentration of $\mathbf{1}_{Cl}$ (eq 4A).

$$[\mathbf{1}_{Cl}] = -\frac{K_x[Cl^-]}{2} + \sqrt{0.25K_x^2[Cl^-]^2 + [Pt]_tK_x[Cl^-]} \quad (4A)$$

Substitution of the expression for $[\mathbf{1}_{Cl}]$ into eq 2A gives the final eq 9, where $A_o = \epsilon_1[\mathbf{1}]$ and $\Delta\epsilon = \epsilon_{Cl} - \epsilon_1$.

Table 6. Crystal Data and Details of the Structure Determination for **2a**

Crystal Data	
empirical formula	$C_{10}H_{14}Cl_3NOPtS$
formula weight (g mol^{-1})	497.726
crystal system	$P\bar{1}$ triclinic
a (Å)	7.1808(7)
b (Å)	8.317(1)
c (Å)	12.725(2)
α (deg)	93.87(1)
β (deg)	98.78(1)
γ (deg)	105.75(1)
V (Å^3)	718.1(2)
Z	2
D(calcd) (g cm^{-3})	2.301
F(000)	497.74
μ(Mo Kα) (cm^{-1})	105.538
crystal size (mm)	0.06 × 0.08 × 0.20
Data Collection	
temperature (K)	293
radiation (Å)	0.71069 (Mo Kα)
θ min, max (deg)	2, 30
scan (deg)	0.90 + 0.35 tan *θ*
data set	0/10, −11/ 11, −17/17
total no. of unique data	3842
no. of obsd data [$I > 3\sigma(I)$]	3733
Refinement	
N_{ref}, N_{par}	3733, 155
R, w*R*	0.0355, 0.0389
w	$1/\sigma^2(F)$
max shift/error	0.00
min, max resd dens (e/Å^3)	−2.16, 1.70

Supporting Information Available: Tables of crystal data, positional parameters, general displacement expressions, results of quantum-chemical calculations, calculated kinetic parameters of eq 11, UV−vis spectra of **2a** recorded under various conditions, dependence of k_{obs1} against [LiCl] for **1b**−**e**, the Eyring plot for k_s, absorbance change vs [LiC] for eq 5, and absorbance change of DMSO in the presence of HCl (PDF). This material is available free of charge via the Internet at http://pubs.acs.org.

JA994342K

(65) Frisch, M. J.; Trucks, G. W.; Schlegel, H. B.; Gill, P. M. W.; Johnson, B. G.; Robb, M. A.; Cheeseman, J. R.; Keith, T. A.; Petersson, G. A.; Montgomery, J. A.; Raghavachari, K.; Al-Laham, M. A.; Zakrzewski, V. G.; Ortiz, J. V.; Foresman, J. B.; Cioslowski, J.; Stefanov, B. B.; Nanayakkara, A.; Challacombe, M.; Peng, C. Y.; Ayala, P. Y.; Chen, W.; Wong, M. W.; Andres, J. L.; Replogle, E. S.; Gomperts, R.; Martin, R. L.; Fox, D. J.; Binkley, J. S.; Defrees, D. J.; Baker, J.; Stewart, J. P.; Head-Gordon, M.; Gonzalez, C.; Pople, J. A. *Gaussian 94* (Revision D.4); Gaussian Inc.: Pittsburgh, PA, 1995.

(66) Hay, P. J.; Wadt, W. R. *J. Chem. Phys.* **1985**, *82*, 270−283.

(67) Wadt, W. R.; Hay, P. J. *J. Chem. Phys.* **1985**, *82*, 284−298.

(68) Hay, P. J.; Wadt, W. R. *J. Chem. Phys.* **1985**, *82*, 299−310.

(69) *International Tables for X-Ray Crystallography*; Kynoch Press: Birmingham, 1974; Vol. IV.